Revisiting hidden-charm pentaquarks from QCD sum rules*

Jia-Bing Xiang(向家兵)[1] Hua-Xing Chen(陈华星)[1;1)] Wei Chen(陈伟)[2;2)] Xiao-Bo Li(李晓博)[1]
Xing-Qun Yao(姚星群)[1] Shi-Lin Zhu(朱世琳)[3,4,5;3)]

[1]School of Physics and Beijing Key Laboratory of Advanced Nuclear Materials and Physics, Beihang University, Beijing 100191, China
[2]School of Physics, Sun Yat-Sen University, Guangzhou 510275, China
[3]School of Physics and State Key Laboratory of Nuclear Physics and Technology, Peking University, Beijing 100871, China
[4]Collaborative Innovation Center of Quantum Matter, Beijing 100871, China
[5]Center of High Energy Physics, Peking University, Beijing 100871, China

Abstract: We revisit hidden-charm pentaquark states $P_c(4380)$ and $P_c(4450)$ using the method of QCD sum rules by requiring the pole contribution to be greater than or equal to 30% in order to better that the one-pole parametrization is valid. We find two mixing currents, and our results suggest that $P_c(4380)$ and $P_c(4450)$ can be identified as hidden-charm pentaquark states having $J^P = 3/2^-$ and $5/2^+$, respectively. However, there still exist other possible spin-parity assignments, such as $J^P = 3/2^+$ and $J^P = 5/2^-$, which must be clarified in further theoretical and experimental studies.

Keywords: exotic hadrons, pentaquark states, QCD sum rules

PACS: 12.39.Mk, 12.38.Lg **DOI:** 10.1088/1674-1137/43/3/034104

1 Introduction

Many exotic hadrons have been discovered in the past decade owing to significant experimental progresses [1], such as the two hidden-charm pentaquark resonances $P_c(4380)$ and $P_c(4450)$ discovered by the LHCb Collaboration [2-5]. More exotic hadrons are likely to be observed in the future by BaBar, Belle, BESIII, CMS, and LHCb experiments, etc. They are new blocks of QCD matter, providing insights to deepen our understanding of the non-perturbative QCD, and their relevant theoretical and experimental studies have opened a new page for hadron physics [6-11].

In the past year, to investigate their nature, $P_c(4380)$ and $P_c(4450)$ have been studied using various methods and models. There are many possible interpretations, such as meson-baryon molecules [12-23], compact diquark-diquark-antiquark pentaquarks [24-27], compact diquark-triquark pentaquarks [28, 29], genuine multiquark states other than molecules [30-35], and kinematical effects related to thresholds and triangle singularity [36-40]. Their productions and decay properties are also interesting [41-53]. More extensive discussions can be found in Refs. [54-56].

The preferred spin-parity assignments for the $P_c(4380)$ and $P_c(4450)$ states were suggested to be $(3/2^-, 5/2^+)$; however, some other assignments, such as $(3/2^+, 5/2^-)$ and $(5/2^+, 3/2^-)$, have also been suggested by the LHCb Collaboration [2]. It is useful to theoretically study all possible assignments to better understand their properties.

In this study, we use the method of QCD sum rule to study the possible spin-parity assignments of $P_c(4380)$ and $P_c(4450)$. However, first, we reinvestigate our previous studies on $P_c(4380)$ and $P_c(4450)$ [57, 58] by requiring the pole contribution (PC) to be greater than or equal to 30% in order to ensure that the one-pole parametrization is valid; this value was just 10% in our previous studies [57, 58]. Note that there have been some experimental data on exotic hadrons; however, they are not sufficient, and more experimental results are necessary to

Received 16 April 2018, Revised 4 December 2018, Published online

* Supported by National Natural Science Foundation of China (11722540, 11261130311), Fundamental Research Funds for the Central Universities, and Foundation for Young Talents in College of Anhui Province (gxyq2018103)

1) E-mail: hxchen@buaa.edu.cn
2) E-mail: chenwei29@mail.sysu.edu.cn
3) E-mail: zhusl@pku.edu.cn

make our theoretical analyses more reliable.

The remainder of this paper is organized as follows: the above reinvestigation is presented in Section 2, numerical analyses are presented in Section 3, the investigation of hidden-charm pentaquark states of $J^P = 3/2^+$ and $J^P = 5/2^-$ are provided in Section 4, and the results will be discussed and summarized in Section 5.

2 QCD sum rules analyses

All the local hidden-charm pentaquark interpolating currents have been systematically constructed in Refs. [57, 58]. Some of these currents were selected to perform QCD sum rule analyses. The results suggest that $P_c(4380)$ and $P_c(4450)$ can be interpreted as hidden-charm pentaquark states composed of anti-charmed mesons and charmed baryons. However, the analyses therein used one criterion, which was not optimized. The condition was that the PC should be greater than 10% to ensure that the one-pole parametrization was valid. This value is not so significant, and accordingly, the question arises whether we can find a larger PC to better ensure one-pole parametrization

In the present study, we try to answer this question to find better (more reliable) QCD sum rule results. In particular, we find the following two mixing currents:

$$\begin{aligned} J_{\mu,3/2-} =& \cos\theta_1 \times \xi_{36\mu} + \sin\theta_1 \times \psi_{9\mu} \\ =& \cos\theta_1 \times [\epsilon^{abc}(u_a^T C\gamma_\nu\gamma_5 d_b)\gamma_\nu\gamma_5 c_c][\bar{c}_d\gamma_\mu\gamma_5 u_d] \\ &+ \sin\theta_1 \times [\epsilon^{abc}(u_a^T C\gamma_\nu u_b)\gamma_\nu\gamma_5 c_c][\bar{c}_d\gamma_\mu d_d], \end{aligned} \tag{1}$$

$$\begin{aligned} J_{\mu\nu,5/2+} =& \cos\theta_2 \times \xi_{15\mu\nu} + \sin\theta_2 \times \psi_{4\mu\nu} \\ =& \cos\theta_2 \times [\epsilon^{abc}(u_a^T C\gamma_\mu\gamma_5 d_b)c_c][\bar{c}_d\gamma_\nu u_d] \\ &+ \sin\theta_2 \times [\epsilon^{abc}(u_a^T C\gamma_\mu u_b)c_c][\bar{c}_d\gamma_\nu\gamma_5 d_d] + \{\mu \leftrightarrow \nu\}, \end{aligned} \tag{2}$$

where $a\cdots d$ are color indices; $\theta_{1/2}$ are two mixing angles; $J_{\mu,3/2-}$ and $J_{\mu\nu,5/2+}$ have the spin-parity $J^P = 3/2^-$ and $5/2^+$, respectively. The four single currents, $\xi_{36\mu}$, $\psi_{9\mu}$, $\xi_{15\mu\nu}$, and $\psi_{4\mu\nu}$, were first constructed in Refs. [57, 58]. We can verify:

1) The current $\xi_{36\mu}$ well couples to the S-wave $[\Lambda_c(1P)\bar{D}_1]$, P-wave $[\Lambda_c(1P)\bar{D}]$, P-wave $[\Lambda_c\bar{D}_1]$, D-wave $[\Lambda_c\bar{D}]$ channels, etc. Here, the $\Lambda_c(1P)$ denotes the $\Lambda_c(2593)$ of $J^P = 1/2^-$ and $\Lambda_c(2625)$ of $J^P = 3/2^-$.

2) The current $\psi_{9\mu}$ well couples to the S-wave $[\Sigma_c\bar{D}^*]$ channel, etc.

3) The current $\xi_{15\mu\nu}$ well couples to the S-wave $[\Lambda_c(1P)\bar{D}^*]$, P-wave $[\Lambda_c\bar{D}^*]$ channels, etc.

4) The current $\psi_{4\mu\nu}$ well couples to the S-wave $[\Sigma_c^*\bar{D}_1]$, P-wave $[\Sigma_c^*\bar{D}]$ channels, etc.

We use the above two mixing currents, $J_{\mu,3/2-}$ and $J_{\mu\nu,5/2+}$, to perform QCD sum rule analyses; the results will be given in the next section. First, we briefly introduce our approach; interested readers can refer to Refs. [59-64] for further details.

First, we assume $J_{\mu,3/2-}$ and $J_{\mu\nu,5/2+}$ couple to physical states through

$$\langle 0|J_{\mu,3/2-}|X_{3/2-}\rangle = f_{X_{3/2-}}u_\mu(p), \tag{3}$$

$$\langle 0|J_{\mu\nu,5/2+}|X_{5/2+}\rangle = f_{X_{5/2+}}u_{\mu\nu}(p), \tag{4}$$

and write the two-point correlation functions as

$$\begin{aligned} &\Pi_{\mu\nu,3/2-}(q^2) \\ &= i\int \mathrm{d}^4x \mathrm{e}^{\mathrm{i}q\cdot x}\langle 0|T\left[J_{\mu,3/2-}(x)\bar{J}_{\nu,3/2-}(0)\right]|0\rangle \\ &= \left(\frac{q_\mu q_\nu}{q^2} - g_{\mu\nu}\right)(\not{q} + M_{X_{3/2-}})\Pi_{3/2-}(q^2) + \cdots, \end{aligned} \tag{5}$$

$$\begin{aligned} &\Pi_{\mu\nu\rho\sigma,5/2+}(q^2) \\ &= i\int \mathrm{d}^4x \mathrm{e}^{\mathrm{i}q\cdot x}\langle 0|T\left[J_{\mu\nu,5/2+}(x)\bar{J}_{\rho\sigma,5/2+}(0)\right]|0\rangle \\ &= \left(g_{\mu\rho}g_{\nu\sigma} + g_{\mu\sigma}g_{\nu\rho}\right)(\not{q} + M_{X_{5/2+}})\Pi_{5/2+}(q^2) + \cdots, \end{aligned} \tag{6}$$

where $\ldots$ contains non-relevant spin components.

Note that if the physical state has the opposite parity, the γ_5-coupling should be used [65-68]. For example, if

$$\langle 0|J_{\mu,3/2-}|X'_{3/2+}\rangle = f_{X'_{3/2+}}\gamma_5 u'_\mu(p), \tag{7}$$

then

$$\begin{aligned} &\Pi_{\mu\nu,3/2+}(q^2) \\ &= i\int \mathrm{d}^4x \mathrm{e}^{\mathrm{i}q\cdot x}\langle 0|T\left[J_{\mu,3/2-}(x)\bar{J}_{\nu,3/2-}(0)\right]|0\rangle \\ &= \left(\frac{q_\mu q_\nu}{q^2} - g_{\mu\nu}\right)(\not{q} - M_{X_{3/2+}})\Pi_{3/2+}(q^2) + \cdots. \end{aligned} \tag{8}$$

Hence, we can compare terms proportional to $\mathbf{1}\times g_{\mu\nu}$ and $\not{q}\times g_{\mu\nu}$ to determine the parity of $X^{(\prime)}_{3/2\pm}$. Accordingly, in the present study, we use terms proportional to $\mathbf{1}\times g_{\mu\nu}$ and $\mathbf{1}\times g_{\mu\rho}g_{\nu\sigma}$ to evaluate masses of X's, which are then compared with those proportional to $\not{q}\times g_{\mu\nu}$ and $\not{q}\times g_{\mu\rho}g_{\nu\sigma}$ to determine their parity.

At the hadron level, we use the dispersion relation to rewrite the two-point correlation function as

$$\Pi(q^2) = \frac{1}{\pi}\int_{s_<}^{\infty}\frac{\mathrm{Im}\Pi(s)}{s - q^2 - i\varepsilon}\mathrm{d}s, \tag{9}$$

where $s_<$ is the physical threshold. Its imaginary part is defined as the spectral function, which can be evaluated by inserting the intermediate hadron states $\sum_n|n\rangle\langle n|$, but adopting the usual parametrization of one-pole dominance for ground state X along with a continuum contribution:

$$\begin{aligned} \rho(s) \equiv& \frac{1}{\pi}\mathrm{Im}\Pi(s) = \sum_n \delta(s - M_n^2)\langle 0|J|n\rangle\langle n|\bar{J}|0\rangle \\ =& f_X^2\delta(s - m_X^2) + \text{continuum}. \end{aligned} \tag{10}$$

At the quark and gluon level, we substitute Eqs. (1-2)

in the two-point correlation functions (5-6),and calculate them using the method of operator product expansion (OPE). In the present study, we evaluate $\rho(s)$ at the leading order on α_s, up to eight dimensions. For this, we calculated the perturbative term, quark condensate $\langle\bar{q}q\rangle$, gluon condensate $\langle g_s^2GG\rangle$, quark-gluon condensate $\langle g_s\bar{q}\sigma Gq\rangle$, and their combinations $\langle\bar{q}q\rangle^2$ and $\langle\bar{q}q\rangle\langle g_s\bar{q}\sigma Gq\rangle$. We find that the $D=4$ term $m_c\langle\bar{q}q\rangle$ and the $D=6$ term $m_c\langle g_s\bar{q}\sigma Gq\rangle$ are important power corrections to the correlation functions. Note that we assumed the vacuum saturation for higher dimensional operators such as $\langle 0|\bar{q}q\bar{q}q|0\rangle \sim \langle 0|\bar{q}q|0\rangle\langle 0|\bar{q}q|0\rangle$, and this can lead to some systematic uncertainties.

Finally, we perform the Borel transform at both the hadron and quark-gluon levels, and express the two-point correlation function as

$$\Pi^{(\mathrm{all})}(M_B^2) \equiv \mathcal{B}_{M_B^2}\Pi(p^2) = \int_{s_<}^{\infty} \mathrm{e}^{-s/M_B^2}\rho(s)\mathrm{d}s. \tag{11}$$

After assuming that the continuum contribution can be well approximated by the OPE spectral density above a threshold value s_0, we obtain the sum rule relation

$$M_X^2(s_0, M_B) = \frac{\int_{s_<}^{s_0} \mathrm{e}^{-s/M_B^2}\rho(s)s\mathrm{d}s}{\int_{s_<}^{s_0} \mathrm{e}^{-s/M_B^2}\rho(s)\mathrm{d}s}. \tag{12}$$

We use the mixing current $J_{\mu,3/2-}$ defined in Eq. (1) to perform sum rule analyses, and the terms proportional to $\mathbf{1}\times g_{\mu\nu}$ are given in Eq. (13), where $t_1=\cos\theta_1$ and $t_2=\sin\theta_1$. The terms proportional to $\not{q}\times g_{\mu\nu}$ are listed in Eq. (14), which are almost the same as the former ones, suggesting that the state coupled by $J_{\mu,3/2-}$ has the spin-parity $J^P=3/2^-$. Similarly, we use $J_{\mu\nu,5/2+}$ defined in Eq. (2) to perform sum rule analyses, and the terms proportional to $\mathbf{1}\times g_{\mu\nu}$ and $\not{q}\times g_{\mu\nu}$ are listed in Eqs. (15) and (16), respectively. We find that its relevant state has the spin-parity $J^P=5/2^+$. These two sum rules will be used to perform numerical analyses in the next section.

$$\begin{aligned}
&\rho_{3/2-,1}(s) = \rho^{\mathrm{pert}}_{3/2-,1}(s) + \rho^{\langle\bar{q}q\rangle}_{3/2-,1}(s) + \rho^{\langle GG\rangle}_{3/2-,1}(s) + \rho^{\langle\bar{q}q\rangle^2}_{3/2-,1}(s) + \rho^{\langle\bar{q}Gq\rangle}_{3/2-,1}(s) + \rho^{\langle\bar{q}q\rangle\langle\bar{q}Gq\rangle}_{3/2-,1}(s),\\
&\rho^{\mathrm{pert}}_{3/2-,1}(s) = \frac{m_c}{3932160\pi^8}\int_{\alpha_{\min}}^{\alpha_{\max}}\mathrm{d}\alpha\int_{\beta_{\min}}^{\beta_{\max}}\mathrm{d}\beta\left\{\left[(\alpha+\beta)m_c^2-\alpha\beta s\right]^5\times\frac{(1-\alpha-\beta)^3(\alpha+\beta+3)\left(11t_1^2-4t_1t_2+24t_2^2\right)}{\alpha^5\beta^4}\right\},\\
&\rho^{\langle\bar{q}q\rangle}_{3/2-,1}(s) = \frac{m_c^2\langle\bar{q}q\rangle}{3072\pi^6}\int_{\alpha_{\min}}^{\alpha_{\max}}\mathrm{d}\alpha\int_{\beta_{\min}}^{\beta_{\max}}\mathrm{d}\beta\left\{\left[(\alpha+\beta)m_c^2-\alpha\beta s\right]^3\times\frac{(1-\alpha-\beta)^2\left(3t_1^2-2t_1t_2-6t_2^2\right)}{\alpha^3\beta^3}\right\},\\
&\rho^{\langle GG\rangle}_{3/2-,1}(s) = -\frac{m_c\langle g_s^2GG\rangle}{28311552\pi^8}\int_{\alpha_{\min}}^{\alpha_{\max}}\mathrm{d}\alpha\int_{\beta_{\min}}^{\beta_{\max}}\mathrm{d}\beta\left\{\left[(\alpha+\beta)m_c^2-\alpha\beta s\right]^3\times\left(\frac{432(1-\alpha-\beta)(\alpha+\beta+1)\left(t_1^2+2t_2^2\right)}{\alpha^3\beta^2}\right.\right.\\
&\quad-\frac{12(1-\alpha-\beta)^2(\alpha+\beta-4)\left(7t_1^2-4t_1t_2+16t_2^2\right)}{\alpha^3\beta^3}-\frac{36(1-\alpha-\beta)^2(\alpha+\beta+2)\left(7t_1^2-4t_1t_2+16t_2^2\right)}{\alpha^4\beta^2}\\
&\quad\left.+\frac{(1-\alpha-\beta)^3(\alpha+\beta-5)(t_1^2+4t_1t_2)}{\alpha^4\beta^3}-\frac{6(1-\alpha-\beta)^3(\alpha+\beta+3)\left(11t_1^2-4t_1t_2+24t_2^2\right)}{\alpha^5\beta^2}\right)\\
&\quad-6m_c^2\left[(\alpha+\beta)m_c^2-\alpha\beta s\right]^2\times\left(11t_1^2-4t_1t_2+24t_2^2\right)\times\left(\frac{(1-\alpha-\beta)^3(\alpha+\beta+3)}{\alpha^2\beta^4}+\frac{(1-\alpha-\beta)^3(\alpha+\beta+3)}{\alpha^5\beta}\right)\Bigg\},\\
&\rho^{\langle\bar{q}Gq\rangle}_{3/2-,1}(s) = -\frac{m_c^2\langle\bar{q}g_s\sigma\cdot Gq\rangle}{8192\pi^6}\int_{\alpha_{\min}}^{\alpha_{\max}}\mathrm{d}\alpha\int_{\beta_{\min}}^{\beta_{\max}}\mathrm{d}\beta\left\{\left[(\alpha+\beta)m_c^2-\alpha\beta s\right]^2\right.\\
&\quad\left.\times\left(\frac{(1-\alpha-\beta)\left(13t_1^2-8t_1t_2-24t_2^2\right)}{\alpha^2\beta^2}+\frac{2(1-\alpha-\beta)^2t_1t_2}{\alpha^3\beta^2}\right)\right\},\\
&\rho^{\langle\bar{q}q\rangle^2}_{3/2-,1}(s) = \frac{m_c\langle\bar{q}q\rangle^2}{1536\pi^4}\int_{\alpha_{\min}}^{\alpha_{\max}}\mathrm{d}\alpha\int_{\beta_{\min}}^{\beta_{\max}}\mathrm{d}\beta\left\{\left[(\alpha+\beta)m_c^2-\alpha\beta s\right]^2\times\frac{(\alpha+\beta)\left(21t_1^2-4t_1t_2-48t_2^2\right)}{\alpha^2\beta}\right\},\\
&\rho^{\langle\bar{q}q\rangle\langle\bar{q}Gq\rangle}_{3/2-,1}(s) = \frac{m_c\langle\bar{q}q\rangle\langle\bar{q}g_s\sigma\cdot Gq\rangle}{9216\pi^4}\int_{\alpha_{\min}}^{\alpha_{\max}}\mathrm{d}\alpha\int_{\beta_{\min}}^{\beta_{\max}}\mathrm{d}\beta\left\{\left[(\alpha+\beta)m_c^2-\alpha\beta s\right]\right)\\
&\quad\left.\times\left(\frac{3\left(47t_1^2-12t_1t_2-96t_2^2\right)}{\alpha}-\frac{2(\alpha+\beta-2)\left(t_1^2+4t_1t_2\right)}{\alpha\beta}+\frac{3(\alpha+\beta)\left(21t_1^2-4t_1t_2-48t_2^2\right)}{\alpha^2}\right)\right\}\\
&\quad-\frac{m_c\langle\bar{q}q\rangle\langle\bar{q}g_s\sigma\cdot Gq\rangle}{3072\pi^4}\int_{\alpha_{\min}}^{\alpha_{\max}}\mathrm{d}\alpha\left\{\left[m_c^2-\alpha(1-\alpha)s\right]\times\frac{47t_1^2-12t_1t_2-96t_2^2}{\alpha}\right\}.
\end{aligned}\tag{13}$$

$$\rho_{3/2-,2}(s)=\rho^{\rm pert}_{3/2-,2}(s)+\rho^{\langle\bar{q}q\rangle}_{3/2-,2}(s)+\rho^{\langle GG\rangle}_{3/2-,2}(s)+\rho^{\langle\bar{q}q\rangle^2}_{3/2-,2}(s)+\rho^{\langle\bar{q}Gq\rangle}_{3/2-,2}(s)+\rho^{\langle\bar{q}q\rangle\langle\bar{q}Gq\rangle}_{3/2-,2}(s),$$

$$\rho^{\rm pert}_{3/2-,2}(s)=\frac{1}{3932160\pi^8}\int_{\alpha_{\min}}^{\alpha_{\max}}{\rm d}\alpha\int_{\beta_{\min}}^{\beta_{\max}}{\rm d}\beta\left\{\left[(\alpha+\beta)m_c^2-\alpha\beta s\right]^5\right.$$
$$\left.\times\left(\frac{8(1-\alpha-\beta)^3\left(11t_1^2-4t_1t_2+24t_2^2\right)}{\alpha^4\beta^4}-\frac{3(1-\alpha-\beta)^4\left(7t_1^2-4t_1t_2+16t_2^2\right)}{\alpha^4\beta^4}\right)\right\},$$

$$\rho^{\langle\bar{q}q\rangle}_{3/2-,2}(s)=\frac{mc\langle\bar{q}q\rangle}{12288\pi^6}\int_{\alpha_{\min}}^{\alpha_{\max}}{\rm d}\alpha\int_{\beta_{\min}}^{\beta_{\max}}{\rm d}\beta\left\{\left[(\alpha+\beta)m_c^2-\alpha\beta s\right]^3\times\frac{(1-\alpha-\beta)^2\left(21t_1^2-4t_1t_2-48t_2^2\right)}{\alpha^2\beta^3}\right\},$$

$$\rho^{\langle GG\rangle}_{3/2-,2}(s)=-\frac{\langle GG\rangle}{28311552\pi^8}\int_{\alpha_{\min}}^{\alpha_{\max}}{\rm d}\alpha\int_{\beta_{\min}}^{\beta_{\max}}{\rm d}\beta\left\{\left[(\alpha+\beta)m_c^2-\alpha\beta s\right]^3\times\left(\frac{144(1-\alpha-\beta)(\alpha+\beta+1)\left(t_1^2+4t_1t_2\right)}{\alpha^2\beta^2}\right.\right.$$
$$+\frac{96(1-\alpha-\beta)^2\left(5t_1^2-4t_1t_2+12t_2^2\right)}{\alpha^2\beta^3}-\frac{108(1-\alpha-\beta)^2\left(7t_1^2-4t_1t_2+16t_2^2\right)}{\alpha^3\beta^2}+\frac{4(1-\alpha-\beta)^3\left(35t_1^2-52t_1t_2+96t_2^2\right)}{\alpha^2\beta^3}$$
$$\left.+\frac{4(1-\alpha-\beta)^3\left(61t_1^2-44t_1t_2+144t_2^2\right)}{\alpha^3\beta^2}+\frac{(1-\alpha-\beta)^3(\alpha+\beta-5)\left(t_1^2+4t_1t_2\right)}{\alpha^3\beta^2}\right)$$
$$-6mc^2\left[(\alpha+\beta)m_c^2-\alpha\beta s\right]^2\times\left(\frac{8(1-\alpha-\beta)^3\left(11t_1^2-4t_1t_2+24t_2^2\right)}{\alpha\beta^4}+\frac{8(1-\alpha-\beta)^3\left(11t_1^2-4t_1t_2+24t_2^2\right)}{\alpha^4\beta}\right.$$
$$\left.\left.-\frac{3(1-\alpha-\beta)^4\left(7t_1^2-4t_1t_2+16t_2^2\right)}{\alpha\beta^4}-\frac{3(1-\alpha-\beta)^4\left(7t_1^2-4t_1t_2+16t_2^2\right)}{\alpha^4\beta}\right)\right\},$$

$$\rho^{\langle\bar{q}Gq\rangle}_{3/2-,2}(s)=-\frac{mc\langle\bar{q}Gq\rangle}{32768\pi^6}\int_{\alpha_{\min}}^{\alpha_{\max}}{\rm d}\alpha\int_{\beta_{\min}}^{\beta_{\max}}{\rm d}\beta\left\{\left[(\alpha+\beta)m_c^2-\alpha\beta s\right]^2\right.$$
$$\left.\times\left(\frac{8(1-\alpha-\beta)\left(13t_1^2-4t_1t_2-24t_2^2\right)}{\alpha\beta^2}+\frac{(1-\alpha-\beta)^2\left(t_1^2+4t_1t_2\right)}{\alpha^2\beta^2}\right)\right\},$$

$$\rho^{\langle\bar{q}q\rangle^2}_{3/2-,2}(s)=\frac{\langle\bar{q}q\rangle^2}{1536\pi^4}\int_{\alpha_{\min}}^{\alpha_{\max}}{\rm d}\alpha\int_{\beta_{\min}}^{\beta_{\max}}{\rm d}\beta\left\{\left[(\alpha+\beta)m_c^2-\alpha\beta s\right]^2\times\left(\frac{4\left(3t_1^2-2t_1t_2-6t_2^2\right)}{\alpha\beta}-\frac{(1-\alpha-\beta)\left(11t_1^2-4t_1t_2-24t_2^2\right)}{\alpha\beta}\right)\right\},$$

$$\rho^{\langle\bar{q}q\rangle\langle\bar{q}Gq\rangle}_{3/2-,2}(s)=\frac{\langle\bar{q}q\rangle\langle\bar{q}g_s\sigma\cdot Gq\rangle}{9216\pi^4}\int_{\alpha_{\min}}^{\alpha_{\max}}{\rm d}\alpha\int_{\beta_{\min}}^{\beta_{\max}}{\rm d}\beta\left\{\left[(\alpha+\beta)m_c^2-\alpha\beta s\right]\times\left(4\left(18t_1^2-7t_1t_2-36t_2^2\right)+\frac{3\left(11t_1^2-4t_1t_2-24t_2^2\right)}{\alpha}\right.\right.$$
$$\left.\left.-\frac{(3t_1^2-16t_1t_2)}{\beta}-\frac{(1-\alpha-\beta)\left(31t_1^2-12t_1t_2-72t_2^2\right)}{\alpha}-\frac{(1-\alpha-\beta)\left(t_1^2-8t_1t_2\right)}{\beta}\right)\right\}$$
$$-\frac{\langle\bar{q}q\rangle\langle\bar{q}g_s\sigma\cdot Gq\rangle}{3072\pi^4}\int_{\alpha_{\min}}^{\alpha_{\max}}{\rm d}\alpha\left\{\left[m_c^2-\alpha(1-\alpha)s\right]\times\left(25t_1^2-16t_1t_2-48t_2^2\right)\right\}.$$

(14)

$$\rho_{5/2+,1}(s)=\rho^{\rm pert}_{5/2+,1}(s)+\rho^{\langle\bar{q}q\rangle}_{5/2+,1}(s)+\rho^{\langle GG\rangle}_{5/2+,1}(s)+\rho^{\langle\bar{q}q\rangle^2}_{5/2+,1}(s)+\rho^{\langle\bar{q}Gq\rangle}_{5/2+,1}(s)+\rho^{\langle\bar{q}q\rangle\langle\bar{q}Gq\rangle}_{5/2+,1}(s),$$

$$\rho^{\rm pert}_{5/2+,1}(s)=-\frac{m_c}{4915200\pi^8}\int_{\alpha_{\min}}^{\alpha_{\max}}{\rm d}\alpha\int_{\beta_{\min}}^{\beta_{\max}}{\rm d}\beta\left\{\left[(\alpha+\beta)m_c^2-\alpha\beta s\right]^5\times\left(5t_1^2-4t_1t_2+12t_2^2\right)\right.$$
$$\left.\times\left(\frac{10(1-\alpha-\beta)^3(\alpha+\beta+1)}{\alpha^5\beta^4}-\frac{(1-\alpha-\beta)^4(\alpha+\beta+4)}{\alpha^5\beta^4}\right)\right\},$$

$$\rho^{\langle\bar{q}q\rangle}_{5/2+,1}(s)=\frac{mc^2\langle\bar{q}q\rangle}{18432\pi^6}\int_{\alpha_{\min}}^{\alpha_{\max}}{\rm d}\alpha\int_{\beta_{\min}}^{\beta_{\max}}{\rm d}\beta\left\{\left[(\alpha+\beta)m_c^2-\alpha\beta s\right]^3\times\frac{(1-\alpha-\beta)^2(\alpha+\beta+2)(t_1-2t_1)(5t_1+6t_2)}{\alpha^3\beta^3}\right\},$$

$$\rho^{\langle GG\rangle}_{5/2+,1}(s)=\frac{m_c\langle GG\rangle}{35389440\pi^8}\int_{\alpha_{\min}}^{\alpha_{\max}}{\rm d}\alpha\int_{\beta_{\min}}^{\beta_{\max}}{\rm d}\beta\left\{\left[(\alpha+\beta)m_c^2-\alpha\beta s\right]^3\times\left(\frac{360(1-\alpha-\beta)\left(t_1^2+2t_2^2\right)}{\alpha^3\beta^2}\right.\right.$$
$$-\frac{120(1-\alpha-\beta)^2\left(t_1^2+4t_1t_2\right)}{\alpha^3\beta^2}+\frac{90(1-\alpha-\beta)^2\left(3t_1^2-4t_1t_2+8t_2^2\right)}{\alpha^3\beta^3}-\frac{40(1-\alpha-\beta)^3\left(t_1^2-8t_1t_2+6t_2^2\right)}{\alpha^3\beta^2}$$
$$-\frac{20(1-\alpha-\beta)^3\left(t_1^2-4t_1t_2\right)}{\alpha^3\beta^3}-\frac{60(1-\alpha-\beta)^3\left(5t_1^2-4t_1t_2+12t_2^2\right)}{\alpha^5\beta^2}-\frac{5(1-\alpha-\beta)^4\left(7t_1^2-20t_1t_2+24t_2^2\right)}{\alpha^3\beta^3}$$
$$\left.+\frac{6(1-\alpha-\beta)^4(\alpha+\beta+4)\left(5t_1^2-4t_1t_2+12t_2^2\right)}{\alpha^5\beta^2}\right)$$
$$-6mc^2\left[(\alpha+\beta)m_c^2-\alpha\beta s\right]^2\times\left(5t_1^2-4t_1t_2+12t_2^2\right)$$
$$\left.\times\left(\frac{10(1-\alpha-\beta)^3}{\alpha^2\beta^4}+\frac{10(1-\alpha-\beta)^3}{\alpha^5\beta}-\frac{(1-\alpha-\beta)^4(\alpha+\beta+4)}{\alpha^2\beta^4}-\frac{(1-\alpha-\beta)^4(\alpha+\beta+4)}{\alpha^5\beta}\right)\right\},$$

$$\rho^{\langle\bar{q}Gq\rangle}_{5/2+,1}(s)=-\frac{mc^2\langle\bar{q}Gq\rangle}{24576\pi^6}\int_{\alpha_{\min}}^{\alpha_{\max}}{\rm d}\alpha\int_{\beta_{\min}}^{\beta_{\max}}{\rm d}\beta\left\{\left[(\alpha+\beta)m_c^2-\alpha\beta s\right]^2\times\frac{(1-\alpha-\beta)(\alpha+\beta+1)(t_1-2t_1)(17t_1+18t_2)}{\alpha^2\beta^2}\right\},$$

$$\rho^{\langle\bar{q}q\rangle^2}_{5/2+,1}(s)=-\frac{mc\langle\bar{q}q\rangle^2}{768\pi^4}\int_{\alpha_{\min}}^{\alpha_{\max}}{\rm d}\alpha\int_{\beta_{\min}}^{\beta_{\max}}{\rm d}\beta\left\{\left[(\alpha+\beta)m_c^2-\alpha\beta s\right]^2\times\frac{(\alpha+\beta)\left(5t_1^2-4t_1t_2-12t_2^2\right)}{\alpha^2\beta}\right\},$$

$$\rho^{\langle\bar{q}q\rangle\langle\bar{q}Gq\rangle}_{5/2+,1}(s)=-\frac{m_c\langle\bar{q}q\rangle\langle\bar{q}g_s\sigma\cdot Gq\rangle}{4608\pi^4}\int_{\alpha_{\min}}^{\alpha_{\max}}{\rm d}\alpha\int_{\beta_{\min}}^{\beta_{\max}}{\rm d}\beta\left\{\left[(\alpha+\beta)m_c^2-\alpha\beta s\right]\right.$$
$$\left.\times\left(\frac{4(t_1-2t_1)(8t_1+9t_2)}{\alpha}-\frac{(\alpha+\beta)\left(t_1^2-8t_1t_2\right)}{\alpha\beta}\right)\right\}$$
$$+\frac{m_c\langle\bar{q}q\rangle\langle\bar{q}g_s\sigma\cdot Gq\rangle}{1152\pi^4}\int_{\alpha_{\min}}^{\alpha_{\max}}{\rm d}\alpha\left\{\left[m_c^2-\alpha(1-\alpha)s\right]\times\frac{(t_1-2t_1)(8t_1+9t_2)}{\alpha}\right\}. \tag{15}$$

$$\rho_{5/2+,2}(s)=\rho^{\rm pert}_{5/2+,2}(s)+\rho^{\langle\bar{q}q\rangle}_{5/2+,2}(s)+\rho^{\langle GG\rangle}_{5/2+,2}(s)+\rho^{\langle\bar{q}q\rangle^2}_{5/2+,2}(s)+\rho^{\langle\bar{q}Gq\rangle}_{5/2+,2}(s)+\rho^{\langle\bar{q}q\rangle\langle\bar{q}Gq\rangle}_{5/2+,2}(s),$$

$$\rho^{\rm pert}_{5/2+,2}(s)=-\frac{1}{4915200\pi^8}\int_{\alpha_{\rm min}}^{\alpha_{\rm max}}{\rm d}\alpha\int_{\beta_{\rm min}}^{\beta_{\rm max}}{\rm d}\beta\left\{\left[(\alpha+\beta)m_c^2-\alpha\beta s\right]^5\times\left(5t_1^2-4t_1t_2+12t_2^2\right)\right.$$
$$\left.\times\left(\frac{10(1-\alpha-\beta)^3}{\alpha^4\beta^4}-\frac{(1-\alpha-\beta)^4(\alpha+\beta+4)}{\alpha^4\beta^4}\right)\right\},$$

$$\rho^{\langle\bar{q}q\rangle}_{5/2+,2}(s)=\frac{mc\langle\bar{q}q\rangle}{18432\pi^6}\int_{\alpha_{\rm min}}^{\alpha_{\rm max}}{\rm d}\alpha\int_{\beta_{\rm min}}^{\beta_{\rm max}}{\rm d}\beta\left\{\left[(\alpha+\beta)m_c^2-\alpha\beta s\right]^3\times\frac{(1-\alpha-\beta)^2(\alpha+\beta+2)(t_1-2t_1)(5t_1+6t_2)}{\alpha^2\beta^3}\right\},$$

$$\rho^{\langle GG\rangle}_{5/2+,2}(s)=\frac{\langle GG\rangle}{35389440\pi^8}\int_{\alpha_{\rm min}}^{\alpha_{\rm max}}{\rm d}\alpha\int_{\beta_{\rm min}}^{\beta_{\rm max}}{\rm d}\beta\left\{5\left[(\alpha+\beta)m_c^2-\alpha\beta s\right]^3\times\left(\frac{72(1-\alpha-\beta)\left(t_1^2+2t_2^2\right)}{\alpha^2\beta^2}\right.\right.$$
$$-\frac{24(1-\alpha-\beta)^2\left(t_1^2+4t_1t_2\right)}{\alpha^2\beta^2}+\frac{18(1-\alpha-\beta)^2\left(3t_1^2-4t_1t_2+8t_2^2\right)}{\alpha^2\beta^3}-\frac{8(1-\alpha-\beta)^3\left(t_1^2-8t_1t_2+6t_2^2\right)}{\alpha^2\beta^2}$$
$$\left.-\frac{4(1-\alpha-\beta)^3\left(t_1^2+4t_1t_2\right)}{\alpha^2\beta^3}-\frac{(1-\alpha-\beta)^4\left(7t_1^2-20t_1t_2+24t_2^2\right)}{\alpha^2\beta^3}\right)$$
$$-6mc^2\left[(\alpha+\beta)m_c^2-\alpha\beta s\right]^2\times\left(5t_1^2-4t_1t_2+12t_2^2\right)$$
$$\left.\times\left(\frac{10(1-\alpha-\beta)^3}{\alpha\beta^4}+\frac{10(1-\alpha-\beta)^3}{\alpha^4\beta}-\frac{(1-\alpha-\beta)^4(\alpha+\beta+4)}{\alpha\beta^4}-\frac{(1-\alpha-\beta)^4(\alpha+\beta+4)}{\alpha^4\beta}\right)\right\},$$

$$\rho^{\langle\bar{q}Gq\rangle}_{5/2+,2}(s)=-\frac{mc\langle\bar{q}Gq\rangle}{24576\pi^6}\int_{\alpha_{\rm min}}^{\alpha_{\rm max}}{\rm d}\alpha\int_{\beta_{\rm min}}^{\beta_{\rm max}}{\rm d}\beta\left\{\left[(\alpha+\beta)m_c^2-\alpha\beta s\right]^2\times\frac{(1-\alpha-\beta)(\alpha+\beta+1)(t_1-2t_1)(17t_1+18t_2)}{\alpha\beta^2}\right\},$$

$$\rho^{\langle\bar{q}q\rangle^2}_{5/2+,2}(s)=-\frac{\langle\bar{q}q\rangle^2}{768\pi^4}\int_{\alpha_{\rm min}}^{\alpha_{\rm max}}{\rm d}\alpha\int_{\beta_{\rm min}}^{\beta_{\rm max}}{\rm d}\beta\left\{\left[(\alpha+\beta)m_c^2-\alpha\beta s\right]^2\times\frac{(\alpha+\beta)\left(5t_1^2-4t_1t_2-12t_2^2\right)}{\alpha\beta}\right\},$$

$$\rho^{\langle\bar{q}q\rangle\langle\bar{q}Gq\rangle}_{5/2+,2}(s)=-\frac{\langle\bar{q}q\rangle\langle\bar{q}g_s\sigma\cdot Gq\rangle}{4608\pi^4}\int_{\alpha_{\rm min}}^{\alpha_{\rm max}}{\rm d}\alpha\int_{\beta_{\rm min}}^{\beta_{\rm max}}{\rm d}\beta\left\{\left[(\alpha+\beta)m_c^2-\alpha\beta s\right]\times\left(4(t_1-2t_1)(8t_1+9t_2)-\frac{(\alpha+\beta)\left(t_1^2-8t_1t_2\right)}{\beta}\right)\right\}$$
$$+\frac{\langle\bar{q}q\rangle\langle\bar{q}g_s\sigma\cdot Gq\rangle}{1152\pi^4}\int_{\alpha_{\rm min}}^{\alpha_{\rm max}}{\rm d}\alpha\left\{\left[m_c^2-\alpha(1-\alpha)s\right]\times(t_1-2t_1)(8t_1+9t_2)\right\}. \tag{16}$$

3 Numerical analyses

In this section, we use the sum rules for $J_{\mu,3/2-}$ and $J_{\mu\nu,5/2+}$ to perform numerical analyses. The condensates in these equations take the following values [1, 69-76]:

$$\begin{aligned}\langle\bar{q}q\rangle&=-(0.24\pm0.01)^3{\rm GeV}^3,\\ \langle g_s^2GG\rangle&=(0.48\pm0.14){\rm GeV}^4,\\ \langle g_s\bar{q}\sigma Gq\rangle&=M_0^2\times\langle\bar{q}q\rangle,\\ M_0^2&=-0.8{\rm GeV}^2.\end{aligned} \tag{17}$$

We also need the charm and bottom quark masses, for which we use the running mass in the $\overline{MS}$ scheme [1, 69-76]:

$$\begin{aligned}m_c&=1.275\pm0.025{\rm GeV},\\ m_b&=4.18^{+0.04}_{-0.03}{\rm GeV}.\end{aligned} \tag{18}$$

There are three free parameters in Eq. (12): the mixing angles $\theta_{1/2}$, Borel mass M_B, and threshold value s_0. After fine-tuning, we obtain the two mixing angles as $\theta_1=-42°$ and $\theta_2=-45°$. The following three criteria can be satisfied so that reliable sum rule results can be achieved:

1) The first criterion is used to ensure the convergence of the OPE series, i.e., we require the dimension eight to be less than 10%, which can be used to determine the lower limit of the Borel mass:

$${\rm CVG}\equiv\left|\frac{\Pi_{\langle\bar{q}q\rangle\langle g,\bar{q}\sigma Gq\rangle}(\infty,M_B)}{\Pi(\infty,M_B)}\right|\leqslant10\%. \tag{19}$$

2) The second criterion is used to ensure that the one-pole parametrization is valid, i.e., we require the PC to be greater than or equal to 30%, which can be used to determine the upper limit of the Borel mass:

$${\rm PC}(s_0,M_B)\equiv\frac{\Pi(s_0,M_B)}{\Pi(\infty,M_B)}\gtrsim30\%. \tag{20}$$

This criterion better ensures the one-pole parametrization than the criterion used in Refs. [57, 58] which only requires PC $\geqslant$ 10%.

3) The third criterion is that the dependence of both s_0 and M_B dependence of the mass prediction be the weakest in order to obtain reliable mass predictions.

We use the sum rules (13) for the current $J_{\mu,3/2-}$ as an example. Firstly, we fix $\theta_1 = -42°$ and $s_0 = 23$ GeV^2, and show CVG as a function of M_B in the left panel of Fig. 1. We find that the OPE convergence improves with an increase in M_B, and the first criterion requires that $M_B^2 \geqslant 2.89$ GeV^2. We also show the relative contribution of each term in the middle panel of Fig. 1. We find that a good convergence can be achieved in the same region, $M_B^2 \geqslant 2.89$ GeV^2. Next, we still fix $\theta_1 = -42°$ and $s_0 = 23$ GeV^2, and show PC is a function of M_B in the right panel of Fig. 1. We find that the PC decreases with an increase in M_B, and PC = 32% when $M_B^2 = 2.89$ GeV^2. Accordingly, we fix the Borel mass to $M_B^2 = 2.89$ GeV^2 and choose 2.59 GeV^2<M_B^2<3.19 GeV^2 as our working region. We show variations of M_X with respect to M_B in the left panel of Fig. 2 and find that the mass curves are considerably stable around $M_B^2 = 2.89$ GeV^2, as well as inside the Borel window 2.59 GeV^2<M_B^2<3.19 GeV^2.

To use the third criterion to determine s_0, we show variations of M_X with respect to s_0 in the middle panel of Fig. 2, with $\theta_1 = -42°$. The mass curves have a minimum against s_0 when s_0 is approximately 17 GeV^2; therefore, the s_0 dependence of the mass prediction is the weakest at this point. However, the PC at this point is significantly small (only 8%). We find that the PC = 32% at $s_0 = 23$ GeV^2. Moreover, the M_B dependence is the weakest at this point. Accordingly, we fix the threshold value to be $s_0 = 23$ GeV^2 and choose 21 GeV$^2 \leqslant s_0 \leqslant 25$ GeV^2 as our working region.

Finally, we vary θ_1 and repeat the above processes. We show variations of M_X with respect to θ_1 in the right panel of Fig. 2 with $s_0 = 23$ GeV^2 and choosing M_B to satisfy CVG = 10%. We find that the θ_1-dependence of the mass prediction is weak when $\theta_1 \leqslant -40°$. Accordingly, we fix the mixing angle θ_1 to be -42° and choose $\theta_1 = -42 \pm 5°$ as our working region.

For current $J_{\mu,3/2-}$, we fine-tune the mixing angle θ_1 to be −42°, and the working regions are found to be 21 GeV$^2 \leqslant s_0 \leqslant 25$ GeV^2 and 2.59 GeV^2<M_B^2<3.19 GeV^2. We assume the uncertainty of θ_1 to be -42±5°, and we obtain the following numerical results:

$$M_{3/2^-} = 4.40^{+0.17}_{-0.22}\text{GeV},$$
$$f_{3/2^-} = \left(6.5^{+3.2}_{-2.9}\right)\times 10^{-4}\text{GeV}^6, \quad (21)$$

where the central value corresponds to $\theta_1 = -42°$, $s_0 = 23$ GeV^2, and $M_B^2 = 2.89$ GeV^2. The mass uncertainty is due to the mixing angle θ_1, Borel mass M_B, threshold value s_0, charm quark mass m_c, and various condensates [1, 69-76]. We note the following: a) when calculating the mass uncertainty due to the mixing angle θ_1, we have fixed s_0 and M_B; and b) when plotting the mass variation as a function of θ_1, as shown in the right panel of Fig. 2, we have fixed s_0, but while choosing M_B to satisfy CVG = 10%. The above mass value is consistent with the experimental mass of the $P_c(4380)$ [2], and supports it to be a hidden-charm pentaquark having $J^P = 3/2^-$. The current $J_{\mu,3/2-}$ consists of $\xi_{36\mu}$ and $\psi_{9\mu\nu}$, suggesting that the

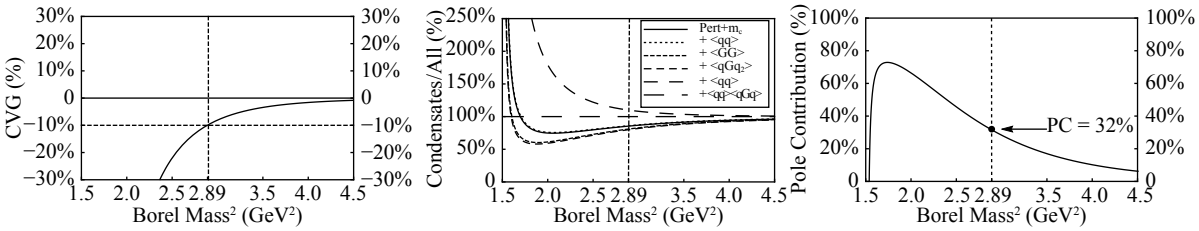

Fig. 1. The left panel shows CVG, defined in Eq. (19), as a function of Borel mass M_B. The middle panel shows the relative contribution of each term on the OPE expansion, as a function of Borel mass M_B. Right panel shows the variation of PC, defined in Eq. (20), as a function of Borel mass M_B. Here we use the current $J_{\mu,3/2-}$ of $J^P = 3/2^-$, and choose $\theta_1 = -42°$ and $s_0 = 23$ GeV^2.

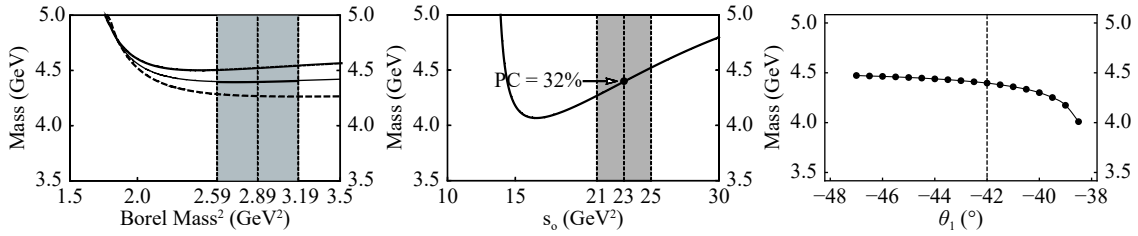

Fig. 2. Variations of $M_{3/2^-}$ with respect to Borel mass M_B (left), threshold value s_0 (middle), and mixing angle θ_1 (right), calculated using the current $J_{\mu,3/2-}$ of $J^P = 3/2^-$. In the left panel, the long-dashed, solid, and short-dashed curves are obtained with $\theta_1 = -42°$ and for $s_0 = 21$, 23, and 25 GeV^2, respectively. In the middle figure, the curve is obtained with $\theta_1 = -42°$ and $M_B^2 = 2.89$ GeV^2. In the right figure, the curve is obtained for $s_0 = 23$ GeV^2 and with M_B satisfying CVG=10%.

$P_c(4380)$ may contain the S-wave $[\Lambda_c(1P)\bar{D}_1]$, P-wave $[\Lambda_c(1P)\bar{D}]$, P-wave $[\Lambda_c\bar{D}_1]$, D-wave $[\Lambda_c\bar{D}]$, S-wave $[\Sigma_c\bar{D}^*]$ components, etc.

Similarly, we investigate the current $J_{\mu\nu,5/2+}$ of $J^P = 5/2^+$. We fine-tune the mixing angle θ_2 to be -45±5°, and the working regions are found to be 21 GeV$^2 \leqslant s_0 \leqslant$25 GeV^2 and 2.31 GeV^2<$M_B^2$<2.91 GeV^2. We show the variations of M_X with respect to M_B, s_0, and θ_2 in Fig. 3, and we obtain the following numerical results:

$$\begin{aligned} M_{5/2^+} &= 4.50^{+0.26}_{-0.24}\text{GeV}, \\ f_{5/2^+} &= \left(5.5^{+3.4}_{-2.4}\right)\times 10^{-4}\text{GeV}^6, \end{aligned} \tag{22}$$

where the central value corresponds to $\theta_2 = -45°$, $s_0 = 23$ GeV^2, and $M_B^2 = 2.61$ GeV^2. The above mass value is consistent with the experimental mass of the $P_c(4450)$ [2], and supports it to be a hidden-charm pentaquark having $J^P = 5/2^+$. The current $J_{\mu\nu,5/2+}$ consists of $\xi_{15\mu}$ and $\psi_{4\mu\nu}$, suggesting that the $P_c(4450)$ may contain the S-wave $[\Lambda_c(1P)\bar{D}^*]$, P-wave $[\Lambda_c\bar{D}^*]$, S-wave $[\Sigma_c^*\bar{D}_1]$, P-wave $[\Sigma_c^*\bar{D}]$ components, etc.

4 Other spin-parity assignments

In this section we follow the same approach to study the hidden-charm pentaquark states of $J^P = 3/2^+$ and $J^P = 5/2^-$. We find the following two currents

$$\begin{aligned} J_{\mu,3/2+} &= \cos\theta_3\times\xi_{35\mu} + \sin\theta_3\times\psi_{10\mu} \\ &= \cos\theta_3\times[\epsilon^{abc}(u_a^T C\gamma_\nu\gamma_5 d_b)\gamma_\nu\gamma_5 c_c][\bar{c}_d\gamma_\mu u_d] \\ &\quad + \sin\theta_3\times[\epsilon^{abc}(u_a^T C\gamma_\nu u_b)\gamma_\nu\gamma_5 c_c][\bar{c}_d\gamma_\mu\gamma_5 d_d], \end{aligned} \tag{23}$$

$$\begin{aligned} J_{\mu\nu,5/2-} &= \cos\theta_4\times\xi_{16\mu\nu} + \sin\theta_4\times\psi_{3\mu\nu} \\ &= \cos\theta_4\times[\epsilon^{abc}(u_a^T C\gamma_\mu\gamma_5 d_b)c_c][\bar{c}_d\gamma_\nu\gamma_5 u_d] \\ &\quad + \sin\theta_4\times[\epsilon^{abc}(u_a^T C\gamma_\mu u_b)c_c][\bar{c}_d\gamma_\nu d_d] \\ &\quad + \{\mu\leftrightarrow\nu\}, \end{aligned} \tag{24}$$

which have structures similar to $J_{\mu,3/2-}$ and $J_{\mu\nu,5/2+}$, respectively. The extracted spectral densities are also similar to previous results:

$$\begin{aligned} \rho_{3/2+,1}(s) =& \rho^{\text{pert}}_{3/2-,1}(s) - \rho^{\langle\bar{q}q\rangle}_{3/2-,1}(s) + \rho^{\langle GG\rangle}_{3/2-,1}(s) \\ & - \rho^{\langle\bar{q}q\rangle^2}_{3/2-,1}(s) + \rho^{\langle\bar{q}Gq\rangle}_{3/2-,1}(s) + \rho^{\langle\bar{q}q\rangle\langle\bar{q}Gq\rangle}_{3/2-,1}(s), \end{aligned} \tag{25}$$

$$\begin{aligned} \rho_{5/2-,1}(s) =& \rho^{\text{pert}}_{5/2+,1}(s) - \rho^{\langle\bar{q}q\rangle}_{5/2+,1}(s) + \rho^{\langle GG\rangle}_{5/2+,1}(s) \\ & - \rho^{\langle\bar{q}q\rangle^2}_{5/2+,1}(s) + \rho^{\langle\bar{q}Gq\rangle}_{5/2+,1}(s) + \rho^{\langle\bar{q}q\rangle\langle\bar{q}Gq\rangle}_{5/2+,1}(s), \end{aligned} \tag{26}$$

where $\rho^{\text{pert}}_{3/2-,1}(s)$, $\rho^{\text{pert}}_{5/2+,1}(s)$, and others have been defined in Eqs. (13) and (15).

First, we study the current $J_{\mu,3/2+}$ of $J^P = 3/2+$. With the same mixing angle θ_1, i.e., $\theta_3 = \theta_1 = -42\pm5°$, the working regions are found to be 21 GeV$^2 \leqslant s_0 \leqslant$25 GeV^2 and 2.58 GeV^2<$M_B^2$<3.18 GeV^2. We show the variations of M_X with respect to s_0 in the left panel of Fig. 4 with $\theta_3 = -42°$, where the mass is extracted to be

$$M_{3/2^+} = 4.40^{+0.14}_{-0.16}\text{GeV}. \tag{27}$$

Then, we study the current $J_{\mu\nu,5/2-}$ of $J^P = 5/2-$. With the same mixing angle θ_2, i.e., $\theta_4 = \theta_2 = -45\pm5°$, the working regions are found to be 21 GeV$^2 \leqslant s_0 \leqslant$25 GeV^2 and 2.20 GeV^2<$M_B^2$<2.80 GeV^2. We show vthe ariations of M_X with respect to s_0 in the right panel of Fig. 4 with $\theta_4 = -45°$, where the mass is extracted to be

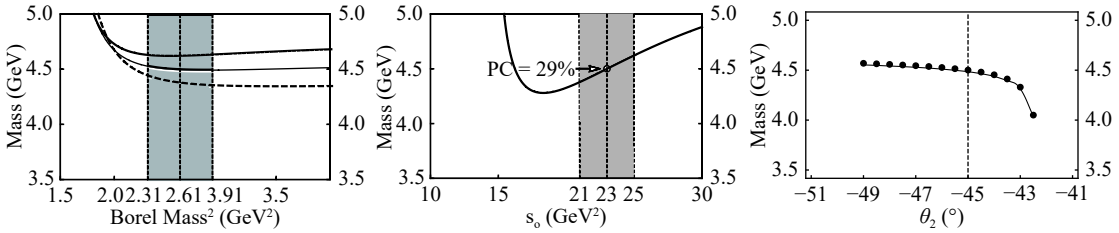

Fig. 3. Variations of $M_{5/2^+}$ with respect to the Borel mass M_B (left), threshold value s_0 (middle), and mixing angle θ_2 (right), calculated using the current $J_{\mu\nu,5/2+}$ of $J^P = 5/2^+$. In the left figure, the long-dashed, solid, and short-dashed curves are obtained with $\theta_2 = -45°$ and for s_0=21, 23 and 25 GeV^2, respectively. In the middle figure, the curve is obtained with $\theta_2 = -45°$ and $M_B^2 = 2.61$ GeV^2. In the right figure, the curve is obtained for $s_0 = 23$ GeV^2 and with M_B satisfying CVG=10%.

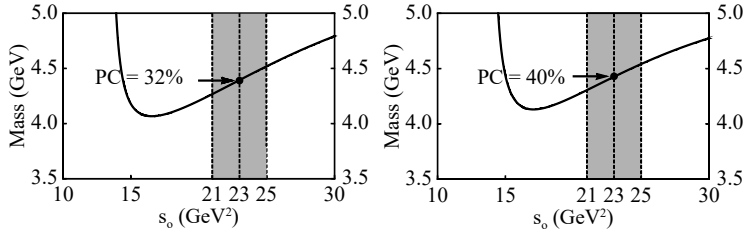

Fig. 4. Variations of $M_{3/2^+}$ (left) and $M_{5/2^-}$ (right) with respect to the threshold value s_0, calculated using the current $J_{\mu,3/2+}$ with $\theta_3 = -42°$ and $J_{\mu\nu,5/2-}$ with $\theta_4 = -45°$, respectively.

$$M_{5/2^-} = 4.43^{+0.26}_{-0.28}\text{GeV}. \quad (28)$$

The above two values are both consistent with the experimental masses of $P_c(4380)$ and $P_c(4450)$ [2], suggesting that their spin-parity assignments can be different from $J^P = 3/2^-$ and $5/2^+$, and further theoretical and experimental efforts are required to clarify their properties.

5 Results and discussions

In this study, we used the method of QCD sum rules to study the hidden-charm pentaquark states $P_c(4380)$ and $P_c(4450)$. We achieved better QCD sum rule results by requiring the PC to be greater than or equal to 30% in order to ensure that the one-pole parametrization was valid; this criterion is stricter than the one used in our previous studies [57, 58]. We found two mixing currents, $J_{\mu,3/2-}$ of $J^P = 3/2^-$ and $J_{\mu\nu,5/2+}$ of $J^P = 5/2^+$. We used them to perform the sum rule analyses, and the masses were extracted to be

$$\begin{aligned} M_{3/2^-} &= 4.40^{+0.17}_{-0.22}\text{GeV}, \\ M_{5/2^+} &= 4.50^{+0.26}_{-0.23}\text{GeV}. \end{aligned} \quad (29)$$

These values are consistent with the experimental masses of $P_c(4380)$ and $P_c(4450)$, suggesting that they can be identified as hidden-charm pentaquark states composed of anti-charmed mesons and charmed baryons: $P_c(4380)$ has $J^P = 3/2^-$ and may contain the S-wave $[\Lambda_c(1P)\bar{D}_1]$, P-wave $[\Lambda_c(1P)\bar{D}]$, P-wave $[\Lambda_c\bar{D}_1]$, D-wave $[\Lambda_c\bar{D}]$, S-wave $[\Sigma_c\bar{D}^*]$ components, etc. $P_c(4450)$ has $J^P = 5/2^+$ and may contain the S-wave $[\Lambda_c(1P)\bar{D}^*]$, P-wave $[\Lambda_c\bar{D}^*]$, S-wave $[\Sigma_c^*\bar{D}_1]$, P-wave $[\Sigma_c^*\bar{D}]$ components, etc.

We follow the same approach to study the hidden-charm pentaquark states of $J^P = 3/2^+$ and $J^P = 5/2^-$, and extract their masses to be

$$\begin{aligned} M_{3/2^+} &= 4.40^{+0.14}_{-0.16}\text{GeV}, \\ M_{5/2^-} &= 4.43^{+0.26}_{-0.28}\text{GeV}. \end{aligned} \quad (30)$$

These values are also consistent with the experimental masses of $P_c(4380)$ and $P_c(4450)$ [2], suggesting that there still exist other possible spin-parity assignments, which should be clarified in further theoretical and experimental studies.

We have also investigated the bottom partners of $P_c(4380)$ and $P_c(4450)$, i.e., the hidden-bottom pentaquark states ($b\bar{b}uud$) of $J^P = 3/2^-$ and $J^P = 5/2^+$. As shown in Fig. 5, their masses are extracted to be

$$\begin{aligned} M_{P_b(3/2^-)} &= 10.83^{+0.26}_{-0.29}\text{GeV}, \\ M_{P_b(5/2^+)} &= 10.85^{+0.24}_{-0.27}\text{GeV}. \end{aligned} \quad (31)$$

We propose to search for them in the future LHCb and BelleII experiments.

In conclusion, we note that there are a considerable systematical uncertainties that are not considered in the present study, such as the vacuum saturation for higher dimensional operators, which is used to calculate the OPE . Moreover, in this study, we used the running charm and bottom quark masses in the $\overline{MS}$ scheme, while sometimes their pole masses were used. Consider thee current $J_{\mu,3/2-}$ as an example: a) if we use $\langle 0|\bar{q}q\bar{q}q|0\rangle = (0.8 \sim 1.2) \times \langle 0|\bar{q}q|0\rangle\langle 0|\bar{q}q|0\rangle$, we would obtain $M_{3/2^-}$=4.34 GeV~4.48 GeV (other uncertainties are not included); b) if we use the pole charm mass $m_c = 1.67$ GeV [1], we would have to shift the mixing angle to be approximately $\theta_1 = -38^\circ$ to arrive at the similar mass $M_{3/2^-} = 4.38$ GeV. Combining the previous uncertainties in Eqs. (21), (22), (27), and (28), we obtain the following result for the mixing current $J_{\mu,3/2-}$ of $J^P = 3/2^-$

$$M_{3/2^-} = 4.40^{+0.19}_{-0.23}\text{GeV}. \quad (32)$$

Similarly, we obtain the following results for the other three mixing currents, $J_{\mu\nu,5/2+}$ of $J^P = 5/2^+$, $J_{\mu,3/2+}$ of $J^P = 3/2^+$, and $J_{\mu\nu,5/2-}$ of $J^P = 5/2^-$:

$$\begin{aligned} M_{5/2^+} &= 4.50^{+0.28}_{-0.27}\text{GeV}, \\ M_{3/2^+} &= 4.40^{+0.16}_{-0.17}\text{GeV}, \\ M_{5/2^-} &= 4.43^{+0.27}_{-0.29}\text{GeV}. \end{aligned} \quad (33)$$

The above (systematical) uncertainties are significant, suggesting that we still know little about exotic hadrons, and further experimental and theoretical studies are necessary to understand them well.

We thank Professor Nikolai Kochelev for helpful discussions.

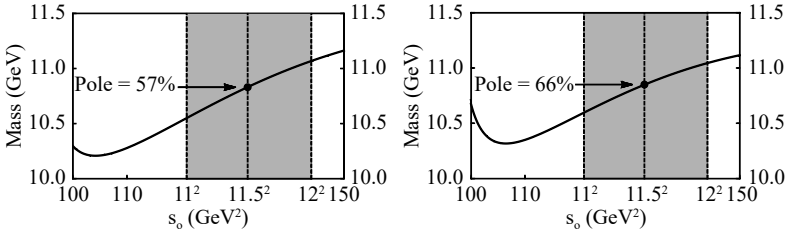

Fig. 5. Variations of $M_{P_b(3/2^-)}$ (left) and $M_{P_b(5/2^+)}$ (right) with respect to the threshold value s_0, calculated using the current $J^{b\bar{b}uud}_{\mu,3/2-}$ with $\theta_1 = -42^\circ$ and $J^{b\bar{b}uud}_{\mu\nu,5/2+}$ with $\theta_2 = -45^\circ$, respectively.

References

1 C. Patrignani et al (Particle Data Group), Chin. Phys. C, **40**: 100001 (2016)
2 R. Aaij et al (LHCb Collaboration), Phys. Rev. Lett., **115**: 072001 (2015), arXiv:1507.03414 [hep-ph]
3 R. Aaij et al (LHCb Collaboration), Chin. Phys. C, **40**: 011001 (2016), arXiv:1509.00292 [hep-ph]
4 R. Aaij et al (LHCb Collaboration), Phys. Rev. Lett., **117**: 082003 (2016), arXiv:1606.06999 [hep-ph]
5 R. Aaij et al (LHCb Collaboration), Phys. Rev. Lett., **119**: 062001 (2017), arXiv:1704.07900 [hep-ph]
6 H. X. Chen, W. Chen, X. Liu, and S. L. Zhu, Phys. Rept., **639**: 1 (2016), arXiv:1601.02092 [hep-ph]
7 H. X. Chen, W. Chen, X. Liu, Y. R. Liu, and S. L. Zhu, Rept. Prog. Phys., **80**: 076201 (2017), arXiv:1609.08928 [hep-ph]
8 A. Esposito, A. Pilloni, and A. D. Polosa, Phys. Rept., **668**: 1 (2016), arXiv:1611.07920 [hep-ph]
9 F. K. Guo, C. Hanhart, U. G. Meissner, Q. Wang, Q. Zhao, and B. S. Zou, Rev. Mod. Phys., **90**: 015004 (2018), arXiv:1705.00141 [hep-ph]
10 A. Ali, J. S. Lange, and S. Stone, Prog. Part. Nucl. Phys., **97**: 123 (2017), arXiv:1706.00610 [hep-ph]
11 S. L. Olsen, T. Skwarnicki, and D. Zieminska, Rev. Mod. Phys., **90**: 015003 (2018), arXiv:1708.04012 [hep-ph]
12 J. J. Wu, R. Molina, E. Oset, and B. S. Zou, Phys. Rev. Lett., **105**: 232001 (2010), arXiv:1007.0573 [hep-ph]
13 Z. C. Yang, Z. F. Sun, J. He, X. Liu, and S. L. Zhu, Chin. Phys. C, **36**: 6 (2012), arXiv:1105.2901 [hep-ph]
14 W. L. Wang, F. Huang, Z. Y. Zhang, and B. S. Zou, Phys. Rev. C, **84**: 015203 (2011), arXiv:1101.0453 [hep-ph]
15 C. W. Xiao, J. Nieves, and E. Oset, Phys. Rev. D, **88**: 056012 (2013), arXiv:1304.5368 [hep-ph]
16 M. Karliner and J. L. Rosner, Phys. Rev. Lett., **115**: 122001 (2015), arXiv:1506.06386 [hep-ph]
17 R. Chen, X. Liu, X. Q. Li, and S. L. Zhu, Phys. Rev. Lett., **115**: 132002 (2015), arXiv:1507.03704 [hep-ph]
18 J. He, Phys. Lett. B, **753**: 547 (2016), arXiv:1507.05200 [hep-ph]
19 T. F. Carames, C. E. Fontoura, G. Krein, K. Tsushima, J. Vijande, and A. Valcarce, Phys. Rev. D, **94**: 034009 (2016), arXiv:1608.04040 [hep-ph]
20 Q. F. Lu and Y. B. Dong, Phys. Rev. D, **93**: 074020 (2016), arXiv:1603.00559 [hep-ph]
21 K. Azizi, Y. Sarac, and H. Sundu, Phys. Rev. D, **95**: 094016 (2017), arXiv:1612.07479 [hep-ph]
22 Y. Dong, A. Faessler, and V. E. Lyubovitskij, Prog. Part. Nucl. Phys., **94**: 282 (2017)
23 R. Chen, J. He, and X. Liu, Chin. Phys. C, **41**: 103105 (2017), arXiv:1609.03235 [hep-ph]
24 L. Maiani, A. D. Polosa, and V. Riquer, Phys. Lett. B, **749**: 289 (2015), arXiv:1507.04980 [hep-ph]
25 R. F. Lebed, Phys. Lett. B, **749**: 454 (2015), arXiv:1507.05867 [hep-ph]
26 Z. G. Wang, Eur. Phys. J. C, **76**: 70 (2016), arXiv:1508.01468 [hep-ph]
27 V. R. Debastiani and F. S. Navarra, arXiv: 1706.07553 [hep-ph].
28 R. Zhu and C. F. Qiao, Phys. Lett. B, **756**: 259 (2016), arXiv:1510.08693 [hep-ph]
29 J.-M. Richard, A. Valcarce, and J. Vijande, Phys. Lett. B, **774**: 710 (2017), arXiv:1710.08239 [hep-ph]
30 A. Mironov and A. Morozov, JETP Lett., **102**: 271 (2015), arXiv:1507.04694 [hep-ph]
31 C. Deng, J. Ping, H. Huang, and F. Wang, Phys. Rev. D, **95**: 014031 (2017), arXiv:1608.03940 [hep-ph]
32 S. Takeuchi and M. Takizawa, Phys. Lett. B, **764**: 254 (2017), arXiv:1608.05475 [hep-ph]
33 J. Wu, Y. R. Liu, K. Chen, X. Liu, and S. L. Zhu, Phys. Rev. D, **95**: 034002 (2017), arXiv:1701.03873 [hep-ph]
34 W. Park, A. Park, S. Cho, and S. H. Lee, Phys. Rev. D, **95**: 054027 (2017), arXiv:1702.00381 [hep-ph]
35 H. Li, Z. X. Wu, C. S. An, and H. Chen, Chin. Phys. C, **41**: 124104 (2017)
36 F. K. Guo, U. G. Meissner, W. Wang, and Z. Yang, Phys. Rev. D, **92**: 071502 (2015), arXiv:1507.04950 [hep-ph]
37 X. H. Liu, Q. Wang, and Q. Zhao, Phys. Lett. B, **757**: 231 (2016), arXiv:1507.05359 [hep-ph]
38 M. Bayar, F. Aceti, F. K. Guo, and E. Oset, Phys. Rev. D, **94**: 074039 (2016), arXiv:1609.04133 [hep-ph]
39 T. F. Carames and A. Valcarce, Phys. Lett. B, **758**: 244 (2016), arXiv:1605.04428 [hep-ph]
40 J. J. Xie and F. K. Guo, Phys. Lett. B, **774**: 108 (2017), arXiv:1709.01416 [hep-ph]
41 Y. Huang, J. He, H. F. Zhang, and X. R. Chen, J. Phys. G, **41**: 115004 (2014), arXiv:1305.4434 [hep-ph]
42 G. N. Li, X. G. He, and M. He, JHEP, **1512**: 128 (2015), arXiv:1507.08252 [hep-ph]
43 Q. Wang, X. H. Liu, and Q. Zhao, Phys. Rev. D, **92**: 034022 (2015), arXiv:1508.00339 [hep-ph]
44 Q. F. Lu, X. Y. Wang, J. J. Xie, X. R. Chen, and Y. B. Dong, Phys. Rev. D, **93**: 034009 (2016), arXiv:1510.06271 [hep-ph]
45 G. J. Wang, L. Ma, X. Liu, and S. L. Zhu, Phys. Rev. D, **93**: 034031 (2016), arXiv:1511.04845 [hep-ph]
46 Y. K. Hsiao and C. Q. Geng, Phys. Lett. B, **751**: 572 (2015), arXiv:1508.03910 [hep-ph]
47 H. X. Chen, L. S. Geng, W. H. Liang, E. Oset, E. Wang, and J. J. Xie, Phys. Rev. C, **93**: 065203 (2016), arXiv:1510.01803 [hep-ph]
48 E. Wang, H. X. Chen, L. S. Geng, D. M. Li, and E. Oset, Phys. Rev. D, **93**: 094001 (2016), arXiv:1512.01959 [hep-ph]
49 S. H. Kim, H. C. Kim, and A. Hosaka, Phys. Lett. B, **763**: 358 (2016), arXiv:1605.02919 [hep-ph]
50 Y. Huang, J. J. Xie, J. He, X. Chen, and H. F. Zhang, Chin. Phys. C, **40**: 124104 (2016), arXiv:1604.05969 [hep-ph]
51 S. Y. Li, Y. R. Liu, Y. N. Liu, Z. G. Si, and X. F. Zhang, Commun. Theor. Phys., **69**: 291 (2018), arXiv:1706.04765 [hep-ph]
52 C. W. Xiao, Phys. Rev. D, **95**: 014006 (2017), arXiv:1609.02712 [hep-ph]
53 W. Wang, Chin. Phys. C, **42**: 043103 (2018), arXiv:1709.10382 [hep-ph]
54 T. J. Burns, Eur. Phys. J. A, **51**: 152 (2015), arXiv:1509.02460 [hep-ph]
55 N. N. Scoccola, D. O. Riska, and M. Rho, Phys. Rev. D, **92**: 051501 (2015), arXiv:1508.01172 [hep-ph]
56 Z. H. Guo and J. A. Oller, Phys. Rev. D, **93**: 096001 (2016), arXiv:1508.06400 [hep-ph]
57 H. X. Chen, W. Chen, X. Liu, T. G. Steele, and S. L. Zhu, Phys. Rev. Lett., **115**: 172001 (2015), arXiv:1507.03717 [hep-ph]
58 H. X. Chen, E. L. Cui, W. Chen, X. Liu, T. G. Steele, and S. L. Zhu, Eur. Phys. J. C, **76**: 572 (2016), arXiv:1602.02433 [hep-ph]
59 M. A. Shifman, A. I. Vainshtein, and V. I. Zakharov, Nucl. Phys. B, **147**: 385 (1979)
60 L. J. Reinders, H. Rubinstein, and S. Yazaki, Phys. Rept., **127**: 1 (1985)
61 M. Nielsen, F. S. Navarra, and S. H. Lee, Phys. Rept., **497**: 41 (2010), arXiv:0911.1958 [hep-ph]
62 H. X. Chen, A. Hosaka, and S. L. Zhu, Phys. Rev. D, **74**: 054001 (2006), arXiv:hep-ph/0604049 [hep-ph]
63 W. Chen and S. L. Zhu, Phys. Rev. D, **83**: 034010 (2011), arXiv:1010.3397 [hep-ph]
64 H. X. Chen, Q. Mao, W. Chen, X. Liu, and S. L. Zhu, Phys. Rev. D, **96**: 031501 (2017), arXiv:1707.01779 [hep-ph]
65 Y. Chung, H. G. Dosch, M. Kremer, and D. Schall, Nucl. Phys. B, **197**: 55 (1982)
66 D. Jido, N. Kodama, and M. Oka, Phys. Rev. D, **54**: 4532 (1996), arXiv:hep-ph/9604280 [hep-ph]
67 Y. Kondo, O. Morimatsu, and T. Nishikawa, Nucl. Phys. A, **764**:

303 (2006), arXiv:hepph/0503150 [hep-ph]
68 K. Ohtani, P. Gubler, and M. Oka, Phys. Rev. D, **87**: 034027 (2013), arXiv:1209.1463 [hep-ph]
69 K. C. Yang, W. Y. P. Hwang, E. M. Henley, and L. S. Kisslinger, Phys. Rev. D, **47**: 3001 (1993)
70 S. Narison, Nucl. Phys. B, **509**: 312 (1998), arXiv:hep-ph/9612457 [hep-ph]
71 S. Narison, Camb. Monogr. Part. Phys. Nucl. Phys. Cosmol., **17**: 1 (2002)
72 M. Eidemuller and M. Jamin, Phys. Lett. B, **498**: 203 (2001), arXiv:hep-ph/0010334 [hep-ph]
73 V. Gimenez, V. Lubicz, F. Mescia, V. Porretti, and J. Reyes, Eur. Phys. J. C, **41**: 535 (2005), arXiv:hep-lat/0503001 [hep-ph]
74 M. Jamin, Phys. Lett. B, **538**: 71 (2002), arXiv:hep-ph/0201174 [hep-ph]
75 B. L. Ioffe and K. N. Zyablyuk, Eur. Phys. J. C, **27**: 229 (2003), arXiv:hep-ph/0207183 [hep-ph]
76 P. Colangelo and A. Khodjamirian, *At the Frontier of Particle Physics/Handbook of QCD*, Singapore, World Scientific, 2001, 1495